Catalysis Today 418 (2023) 114086

Contents lists available at ScienceDirect

Catalysis Today

journal homepage: www.elsevier.com/locate/cattod

Sustainable isosorbide production by a neat one-pot MW-assisted catalytic glucose conversion

M. Belluati [a], S. Tabasso [a,*], F. Bucciol [a], T. Tabanelli [b], F. Cavani [b], G. Cravotto [a], M. Manzoli [a,*]

[a] Department of Drug Science and Technology and NIS Interdepartmental Center, University of Turin, V. Pietro Giuria 9, 10125 Torino, Italy
[b] Department of Industrial Chemistry "Toso Montanari", University of Bologna, Viale del Risorgimento 4, 40136 Bologna, Italy

ARTICLE INFO

Keywords:
Isosorbide
One-pot conversion
Zeolites
Microwaves
Ruthenium-based heterogeneous catalysts

ABSTRACT

In the context of exploitation of new biomass-derived platform chemicals, isosorbide (1,4:3,6-dianhydro-D-sorbitol), obtained by the two-fold dehydration of sorbitol, is gaining increasing interest in several potential industrial applications. Seeking for more sustainable, efficient, and economically competitive green processes, the use of heterogeneous catalysts under microwave (MW) irradiation has been adopted for the development of a neat one-pot process from glucose. MW-assisted catalytic processes have shown the potential to reduce the reaction time and improve the selectivity, due to the interaction of MW with the reaction medium through the production of hot spots on the catalyst surface. Ru/C, Ru/Al_2O_3 and Ru/TiO_2 were tested for glucose hydrogenation to sorbitol, while the dehydration step was favored by the addition of β Zeolites (360:1 SiO_2:Al_2O_3) allowing high isosorbide selectivity (>85 %). An extended structural and morphological characterization before and after the catalytic tests allowed to establish structure-activity relationships. Yields up to 47.1 % have been obtained directly from glucose in 1.5 h, achieving a considerable reduction of reaction time without the use of a solvent. thus paving the way for further investigations on biomass conversion into value-added products.

With this aim, direct isosorbide production from milled cellulose was investigated. While the isosorbide yields still need to be improved, the dual role of formic acid both as acid catalyst for cellulose hydrolysis and H-donor for the reduction step was promisingly clarified.

1. Introduction

Despite having clearly boosted economic and social development during the XX century, the constant exploitation and depletion of fossil resources brought health hazards and environmental threats, thus recently driving research efforts towards alternatives to refinery processes. In this context, the use of renewable sources as raw material and the reduction of the environmental footprint of chemical reactions gained an increasing importance.

Due to their global availability and carbon neutrality, lignocellulosic biomasses are considered a promising alternative to fossil resources, considering the *plethora* of platform chemicals that can be obtained from their macro-components: cellulose, hemicellulose and lignin [1]. As indicated in the list elaborated from the United States Department of Energy, sorbitol is one of the most a promising platform chemical that can be obtained from cellulose conversion [2,3].

Sorbitol is involved in several branches of the chemical industry [4], and is also a precursor for dehydration processes, producing high-value products as isosorbide (1,4–3,6-dianhydro-D-sorbitol). Isosorbide global production has reached 10^4 tons in 2020, with a 413.3 million USD expected to reach 700 million USD by 2027 by means of a 7.9 % compound annual growth rate (CAGR) [5].

Isosorbide is described as heat-stable at temperatures up to 270 °C and acid withstanding, thus tolerating the use of acidic catalysts for its synthesis [6,7]. The possibility of further derivatization of its two hydroxylic groups make isosorbide a target molecule of special interest for biorefinery development, stating increasing interest towards its role as a new platform chemical.

Nowadays, isosorbide is mainly used to produce isosorbide-5-mononitrate, a drug for cardiovascular diseases. Review works from Saxon and Aricò have however highlighted the potential role of isosorbide as a building block for next-generation polymers and surfactants, as well for the synthesis of green solvents and organo-catalysts [8,9].

The generally recognized procedure for the production of isosorbide involves a two-step process, involving glucose hydrogenation to sorbitol

* Corresponding authors.
E-mail addresses: silvia.tabasso@unito.it (S. Tabasso), maela.manzoli@unito.it (M. Manzoli).

https://doi.org/10.1016/j.cattod.2023.114086
Received 14 December 2022; Received in revised form 1 March 2023; Accepted 5 March 2023
Available online 6 March 2023

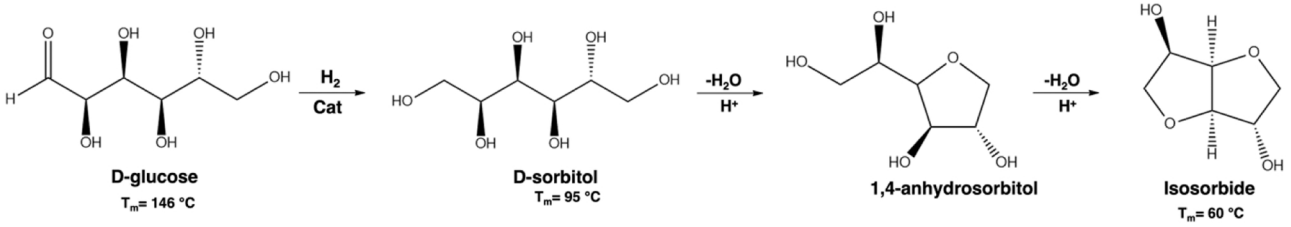

Scheme 1. Glucose hydrogenation to sorbitol in the presence of a heterogeneous catalyst and acid-catalyzed two-fold cyclodehydration to isosorbide. The melting points (T_m) of the reactants and the products are also reported.

and an acid-catalyzed two-fold cyclodehydration, as reported in Scheme 1.

The role of noble metals (e.g. Pt, Ru) in heterogeneous catalysis has been widely explored in literature [10,11]. The role of different heterogeneous catalysts on the hydrogenation of glucose to sorbitol, assessing the higher activity of Ru compared to Pt, Pd and Ni and the challenges involved into the development of sustainable procedures for glucose conversion (reaction conditions, catalyst design and reusability) were reported [12].

After a single cyclodehydration of sorbitol, the formation of 1,4-anhydrosorbitol (1,4-sorbitan) is observed (Scheme 1) along with and other anhydroexitols (e.g. 2,5 and 1,5-anhydrosorbitol in negligible amounts). 1,4-sorbitan represents one of two intermediates but can be also used as a precursor for the production of surfactants and food additives [13]. After the second cyclodehydration, 1,4- and 3,6- sorbitans result into isosorbide formation, whereas other reaction intermediates can undergo degradation to humins [14]. The use of enabling technologies such as MW irradiation, could help to overcome degradation issues, as dielectric heating is more homogeneous than convective heating, allowing shorter reaction times and higher product selectivity [15].

A kinetic analysis by Yamaguchi et al. shown that temperatures up to 260 °C are required to achieve double cyclization of sorbitol in aqueous solution [16]. The use of high temperatures, however, exposes the system to degradation processes [17].

In a state-of-the-art contribution from Delbecq et al. [6], the catalytic production of isosorbide from sorbitol has been extensively reviewed, highlighting the issues affecting homogeneous acid catalysis, such as equipment corrosion, waste disposal, products separation and use of mineral acids (e.g. H_2SO_4). Other than representing a facile and more sustainable approach, the adoption of heterogeneous catalysis has reportedly brought comparable catalytic performances with homogeneous catalysis. Specifically, when employed in sorbitol cyclodehydration, acidic resins proved able to afford yields higher than 80 % [18–21], while sulfonated and sulfated titania reached > 70 % isosorbide yields [22].

A general requirement for catalytic sorbitol dehydration is the presence of Brønsted acidity rather than Lewis acidity [14,23]. Among the heterogeneous catalysts employed for sorbitol dehydration, the use of zeolites as dehydrating agent has recently emerged, thanks to their large availability, benignity,and low cost. Kobayashi and coworkers published a solventless zeolite-catalyzed sorbitol dehydrationproviding a complete screening of different zeolites reactivity. A mechanistic study on the reaction, moreover, demonstrated the key role of acidic sites on the internal hydrophobic zeolite surface, resulting in a 76 % isosorbide yield after 2 h at 127 °C using the mildly acidic H-β zeolites (Si/Al=75) [24]. Solventless conditions are desirable both from an environmental point of view and to boost H_2O removal [22,25,26].

Very few works treating direct synthesis of isosorbide from glucose are reported in literature. In 2016, Barbaro et al. described isosorbide catalytic production from glucose with the use of Ru-supported acid resins and water as reaction medium and long reaction times (48 h, 30 bar H_2) [19]. Despite a final 84.9 % isosorbide yield, the high E-factor value of the overall process and poor reusability of the catalytic system affected the sustainability on the process. Isosorbide continuous production from an aqueous glucose solution was accomplished by using two fixed bed reactors, respectively containing a Ni-based catalyst (hydrogenation) and a H-β zeolite (Si:Al=75) (dehydration) [27]. However, high temperatures were required to achieve a 54 % isosorbide molar yield, and the use of a Ni-based catalyst with a 35 % Ni loading still represents an issue to be dealt with.

Direct cellulose conversion is considered an appealing process for biorefinery development [28]. However, high isosorbide yields were often achieved by using homogeneous acid catalysts (e.g HCl, H_2SO_4) and heteropolyacids (e.g. $H_4SiW_{12}O_{40}$), but resulting in limited sustainability of the process. On the other hand, the use of Ru-based heterogeneous catalysts, despite affording promising results, required a strict pH control either to achieve cellulose depolymerization or avoid the products degradation. Bifunctional catalysts, such as a Ru-supported mesoporous niobium phosphate, were described, affording a complete cellulose conversion and a 52 % isosorbide yield [29].

Considering the actual development, the most significant drawbacks regarding the use of heterogeneous catalysts for direct cellulose conversion are represented by the formation of degradation products, drastic reaction conditions and consequent catalyst deactivation, which make the development of these processes not yet mature. The challenge for the development of a sustainable process greatly relies on cellulose hydrolysis and glucose hydrogenation, since the subsequent sorbitol cyclodehydration is reportedly carried out more easily [6,28]. As indicated by Shrotri and colleagues, cellulose depolymerization by means of homogeneous acidic catalysis represents a solution with limited perspectives and questionable sustainability [30]. In this context, coupling the acidity of formic acid for cellulose hydrolysis [31] with its known H-Donor properties [32,33], could represent a decisive leap towards the establishment of a reliable cellulose-based production of isosorbide.

Herein, the MW-assisted solventless one-pot conversion of glucose to isosorbide is reported. Different Ru-based catalysts were tested for the hydrogenation step. Commercial H-Y (30:1 SiO_2:Al_2O_3) and low-acidity H-β zeolites (360:1 SiO_2:Al_2O_3) were used to boost the further sorbitol dehydration.

Furthermore, formic acid was tested for the direct cellulose conversion as both acid catalyst for cellulose depolymerization and H-donor for glucose hydrogenation, affording promising preliminary results.

2. Materials and methods

All chemicals and solvents were purchased from commercial suppliers and used without further purification. Commercial H-Y (SiO_2:Al_2O_3 ratio equal to 30 and 5) and H-β (360:1 SiO_2:Al_2O_3) zeolites were purchased from Alfa Aesar. Microcrystalline cellulose was purchased from Sigma Aldrich and was treated with ball mill for 1 h with a 550 rpm (Retsch PM100 High Speed Planetary Ball Mill).

2.1. Preparation of the catalysts

Commercial supports were used as received: AC (NORIT SX 1 G, lot # A-10536) with a Specific Surface Area (*SSA*) of 1045 m^2/g, Al_2O_3 (Puralox SCFa-140, Sasol), *SSA*= 140 m^2/g and TiO_2 (Titania Crystal

Active DT51), *SSA*= 80 m^2/g. The preparation of the supported 3 wt % Ru catalysts was performed as follows: 0.2318 g of $RuCl_3$ were dissolved in 15 mL of distilled water into a beaker (0.06 M). In a different beaker, 3 g of support were suspended in 60 mL of water. The Ru solution was then slowly added to the support suspension and left under stirring for 2 h. After that, $NaBH_4$ (0.1362 g) was slowly added, and the suspension was left under stirring for 4 additional hours. The solid was then filtered using a Buchner funnel, washed with distilled water and let to dry overnight over the filter at room temperature. Finally, the solid was dried in an oven at 80 °C for 4 h. The prepared catalysts were labelled as Ru/C, Ru/Al_2O_3 and Ru/TiO_2.

2.2. Characterization methods

All as prepared (fresh) catalysts and selected used (after reaction) catalysts were characterized by Transmission Electron Microscopy (TEM) by using a side entry Jeol JEM 3010 (300 kV) microscope equipped with a LaB_6 filament and fitted with X-ray EDS (Energy-Dispersive Spectroscopy) analysis by a Link ISIS 200 detector. The samples, in the form of powders, were deposited on a copper grid, coated with a porous carbon film. All digital micrographs were collected by an Ultrascan 1000 camera and the images were processed by Gatan digital micrograph. Ruthenium particle size distributions were obtained by counting a statistically representative number of particles for each sample (fresh catalysts: 300 counted nanoparticles in the case of Ru/TiO_2, >650 for Ru/C and 550 for Ru/Al_2O_3. Used catalysts: > 200 for Ru/Al_2O_3 + H-β zeolite and 200 for Ru/TiO_2 + H-β zeolite). The mean particle diameter (d_m) was calculated by applying the formula $d_m = \Sigma d_i n_i / \Sigma n_i$ (n_i is the number of particles having diameter d_i). Basing on the obtained particle size distributions, the corresponding metal Specific Surface Area (*SSA*, m^2/g) of the supported Ru particles (supposed to be spherical) was calculated by applying the formula: $3\Sigma n_i r_i^2 / (\rangle_{Ru} \Sigma n_i r_i^3)$ m^2/g, where r_i is the mean radius of the size class containing n_i particles, and $\rangle_{Ru}$ the volumetric mass of Ru (19.3 g/cm^3).

Diffuse Reflectance (DR) UV–Vis-NIR spectra of the fresh catalysts were run at room temperature on a Varian Cary 5000 spectrophotometer, working in the 50,000–4000 cm^{-1} range, with the powders placed in a quartz cell. DR UV–Vis-NIR spectra are reported in the Kubelka-Munk function $f(R_\infty) = (1 - R_\infty)^2/2\,R_\infty$; R_∞=reflectance of an "infinitely thick" layer of the sample.

Powder X-Ray Diffraction (XRD) patterns were collected by using a PW3050/60 X'Pert PRO MPD diffractometer from PANalytical working in Bragg–Brentano geometry, using as a source the high-powered ceramic tube PW3373/10 LFF with a Cu anode (Cu $K_{\alpha 1}$ radiation $\lambda = 1.5406$ Å) equipped with a Ni filter to attenuate K_β. Scattered photons were collected by a real time multiple strip (RTMS) X'celerator detector. Data were collected in the $10° \leq 2\theta \leq 90°$ angular range, with 0.02° 2θ steps. The samples were examined in their as-received form and posed in a spinning sample holder to minimize preferred orientations of crystallites.

Temperature programmed desorption (TPD) of NH_3 was carried out with a Micromeritics Autochem II 2920 instrument equipped with a TCD detector to measure the total acidity of the materials. In a typical experiment, 0.2 g of material was put in a quartz tube and heated up to 400 °C at a rate of 10 ∘C/min in 30 mL/min of pure He flow to clean the catalyst surface from adsorbed water and carbonates. The final temperature was kept for 60 min. After cooling, NH_3 chemisorption was conducted at 100 °C for 20 min by flowing 30 mL/min of 10 % NH_3/He. After chemisorption, all samples were flown with 30 mL/min of He for 60 min to remove the weakly physisorbed probe molecules. Finally, the temperature programmed desorption (TPD) was carried out by heating the sample up to 800 °C at the rate of 10 °C/min and keeping the final temperature for 60 min. NH_3-TPD of acid zeolites have been recorded by adjusting the method described above: all the parameters were kept as already described except for the pretreatment temperature which was increased to 450 °C (kept for 2 h) and the desorption which was followed up to 700 °C with a heating rate of 10 °C/min.

TGA analysis was performed with the use of a Perkin Elmer TGA 4000 instrument. In a typical experiment, about 8 mg of material were placed in a crucible inside the furnace. A 50 °C temperature was set and held for 15 min, and then raised to 500 °C with a 10 °C/min ramp.

FTIR-ATR (Fourier Transformed Infrared Spectroscopy - Attenuated Total Reflectance) analyses were carried out using a Perkin Elmer Spectrum Two instrument, using 16 scans at 1 cm^{-1} and the IR v10.2 software. The spectra were acquired in air in their as synthesized form (fresh catalysts) and after reaction.

2.3. Catalytic tests

All the reactions were performed in a multimode closed-vessel MW reactor (SynthWAVE, Milestone Srl, Italy; MLS GmbH, Germany), with 1500 W power.

For the hydrogenation tests, glucose (100 mg) and the proper amount of catalyst were added into a quartz vial equipped with a magnetic stirrer and heated by MW irradiation at 155 °C, under H_2 pressure (40 bar) and previously optimized magnetic stirring (300 rpm) for the selected time. In the one-pot reaction, the proper amount of zeolite was added at the beginning of the reaction, and after the hydrogenation step, the reaction was carried out under N_2 (30 bar) for the dehydration.

The catalytic transfer hydrogenation tests used the same experimental setup of the previous reactions. For this process, cellulose (100 mg), catalyst (40 mg), zeolite (200 mg) and formic acid (6 mL) were put to react at 200 °C for different reaction times. A 30 bar pressure was used (20 bar H_2 + 10 bar N_2 or 30 bar N_2).

After the reaction, the crude mixture was cooled down, whereupon filtration allowed the separation of the catalyst, which was consequently washed with water and methanol and stored for characterization and recycle tests after being dried (110 °C, 12 h). The reaction media was diluted with water and the resulting aqueous solution was furtherly syringe-filtered, frozen with liquid nitrogen (−196 °C) and freeze-dried (−80 °C, 0.2 mbar). The freeze-dried solid was finally analyzed with gas chromatography.

Samples were dissolved in pyridine and then BSTFA (N,O-bis(trimethylsilyl)trifluoroacetamide) was added for derivatization at 60 °C for 1 h.

Compound identification was carried out with GC-MS (Gas Chromatography – Mass Spectroscopy) Agilent 6980 (Agilent Technologies – USA), an Agilent Network 5973 mass detector and a HP-5 column (length 30 m, *i.d.* 0.25 mm, *f.t.* 0.25 μm). Quantification was performed with GC-FID (Gas Chromatography – Flame Ionization Detector) Agilent 7280 A and the same column used for GC-MS.

The same oven program was used for both techniques: 3 min at 50 °C, 3 °C/min ramp for 50–80 °C heating, 10 °C/min ramp for 80–200 °C heating and 20 °C/min ramp for 200–300 °C heating with 0.50 min equilibration time.

The calibrations curves used to determine sorbitol and isosorbide yield are reported separately (**Figs. SI-1 and SI-2**).

The recovery after reaction (%) was calculated as follows:

$$Recovery(\%) = \frac{m_{rp}}{m_{ir}} \times 100$$

where m_{rp}= mass of recovered products and m_{ir}= mass of initial reagent.

Isosorbide selectivity % was calculated as follows:

$$Selectivity(\%) = \frac{GC - FID\ area_{isosorbide}}{GC - FID\ area_{total}} \times 100$$

Isosorbide yield (%) was calculated as follows:

$$Yield(\%) = \frac{mol_{isosorbide}}{mol_{glucose}} \times 100$$

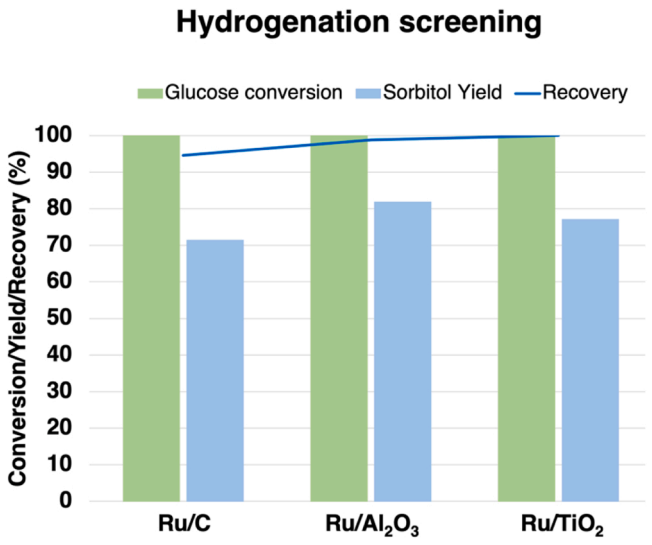

Fig. 1. Catalyst screening for glucose hydrogenation to sorbitol (Reaction conditions: 155 °C, 40 bar H_2, 1 h, glucose:catalyst ratio 4:1).

where $mol_{isosorbide}$= moles of recovered isosorbide after GC-FID quantification and $mol_{glucose}$= moles of glucose initially used.

3. Results and discussion

In order to find the optimized conditions for the one-pot glucose conversion to isosorbide, the two steps involved in the isosorbide production, e.g. glucose hydrogenation to sorbitol and the subsequent acid-catalyzed two-fold cyclodehydration (see Scheme 1) were firstly investigated separately.

3.1. MW-assisted glucose hydrogenation to sorbitol

As for the hydrogenation step, the available literature treating Ru-catalyzed glucose conversion has driven the choice towards the use of these catalytic systems, while Al_2O_3, carbon and TiO_2 were chosen as supports [10–12,34,35]. Regarding the amount of Ru-based catalysts used for the hydrogenation, two glucose:catalyst weight ratios were investigated. On one hand a 4:1 ratio proved its efficacy towards glucose hydrogenation; on the other hand, preliminary tests showed a detrimental effect of a 2.5:1 ratio product recovery and overall sorbitol yield (**Fig. SI-3**).

Moreover, to overcome the mass transfer limitations due to the solventless, i.e. neat, conditions the temperature was set higher than the melting point of glucose (T_m = 146 °C), but not too high to avoid the formation of degradation products. Therefore, the MW-assisted glucose hydrogenation reactions were performed at 155 °C.

The reaction conditions (40 bar H_2, 1 h reaction time) were chosen according to a previous work, affording an almost complete glucose conversion [27]. The formation of glucose isomers was observed, and was already reported in previous studies on sugars hydrogenation [27,36].

The results of the screening of the Ru supported catalysts are shown in Fig. 1. While complete glucose conversion was achieved with all the catalysts, Ru/C afforded 71.4 % sorbitol yield, whereas 81.9 % and 77.0 % yields were obtained in the presence of Ru/Al_2O_3 and Ru/TiO_2, respectively. Moreover, the recovery after reaction was 94.4 % for Ru/C, 98.8 % for Ru/Al_2O_3 and quantitative in the case of Ru/TiO_2. This trend could be ascribed to (i) the much higher surface area of the carbon support (1045 m^2/g) with respect to alumina (140 m^2/g) and titania (80 m^2/g) and (ii) the high adsorption capability of the carbonaceous materials [37], leading to a higher adsorption of the substrate at the surface of the heterogeneous catalyst, which results in a lower recovery.

Compared with the catalytic results obtained with the use of an aqueous reaction media, Ru/C exhibited poorer catalytic performances [12], whereas Ru/Al_2O_3 [38] and Ru/TiO_2 [39] achieved sorbitol yields slightly lower than those reported in the literature.

In order to explain the observed trend in sorbitol yield, a TEM characterization was carried out on all the fresh (as prepared) catalysts to investigate the effect of the support on the Ru nanoparticles dispersion, given the same metal loading. Roundish Ru nanoparticles with d_m= 2.9 ± 1.0 nm have been detected on the carbon support (Fig. 2**a**), being the majority of the particles with size of 2.5 nm and resulting in a Ru *SSA* of 60.8 m^2/g.

However, such nanoparticles appeared not homogeneously distributed within the carbon matrix, since Ru agglomerates were observed in different regions of the sample (as shown in **Fig. SI-4**). This feature indicates that the Ru *SSA* value is probably over-estimated. Conversely, very small Ru nanoparticles (highlighted by harrows in Fig. 2**b**), appearing homogeneously distributed over the alumina and with an average diameter of 1.1 ± 0.5 nm were observed. In this case, the Ru particle size distribution is really narrow, with almost 95 % of the total particles having size < 2.5 nm and about 35 % with size below 1.5 nm, resulting in an exposed Ru *SSA* equal to 135.3 m^2/g.

Similarly to what observed for the Ru/Al_2O_3 catalyst, the metal phase appears homogeneously dispersed on the titania, i.e. no Ru agglomerates were observed. In addition, with respect to Ru/Al_2O_3, a larger average size of the metal nanoparticles was obtained for the fresh Ru/TiO_2 catalyst (d_m= 2.7 ± 0.8 nm, Fig. 2**c**). More in detail, the Ru particle size distribution revealed that a large fraction of the nanoparticles (> 50 %) has size around 2.5 nm.

The absence of nanoparticle agglomerates indicated that the interaction between the Ru nanoparticles and the oxides is stronger than that between the metal and the carbon support. In this frame, alumina proved to be the best support for the metal dispersion efficiency. TPD analyses of the Ru/C catalyst [40] showed that the metal insertion affected the content of carboxylic groups on the activated carbon surface, as well as of phenols and carbonyls, which can indicate that the Ru nanoparticles are interacting with the support through the oxygen-bearing surface groups. Conversely, NH_3-TPD carried out on the Ru/Al_2O_3 catalyst (**Fig. SI-5**) gave rise to a desorption peak at 271 °C with a weak shoulder at 215 °C, due to the presence of two kind of acid sites with different strength. Interestingly, the value of desorbed ammonia obtained from the integration of the peak at 271 °C is equal to 122 μmol NH_3/g, much lower than that found for a γ-alumina similar to that used as a support (826 μmol NH_3/g) [41]. Therefore, the impregnation of the Ru precursor had two effects: i) possible decrease of the surface area of the sample (with consequent decrease of the desorbed ammonia per gram of catalyst) and ii) coverage of the weaker acid sites, corresponding to the peak at 215 °C. However, given the same complete conversion for all catalysts, the observed trend in sorbitol yield, i.e. Ru/C (71.4 %)< Ru/TiO_2 (77.0 %) < Ru/Al_2O_3 (81.9 %), well correlated with the Ru dispersion and *SSA* from TEM, which points out that mainly the size of Ru nanoparticles rules the selectivity particularly when comparing Ru/Al_2O_3 with Ru/C, despite the lower surface area of alumina (140 m^2/g) with respect to the carbon support (1045 m^2/g). In the case of Ru/TiO_2, the obtained yield has an intermediate value, much closer to that attained for Ru/Al_2O_3. This could be related not only to the lower metal dispersion and *SSA*, but also to the lowest surface area of the titania support (80 m^2/g). FTIR-ATR analysis (**Fig. SI-6**) revealed the presence of bands related to carbonate species only on the surface of Ru/TiO_2 accompanied OH groups by less acidic than those detected on Ru/Al_2O_3 (i.e. peak observed at higher frequency), which means that a lower acidity of the titania support with respect to alumina.

As for the electronic properties of the Ru nanoparticles (**Fig. SI-7**), bands at about 23,000 and 16,500 cm^{-1}, due to the plasmon resonance enhanced absorption band of metallic Ru nanoparticles [42], and to $Ru^{\delta+}$ species [43], produced by oxidation of extremely reactive Ru

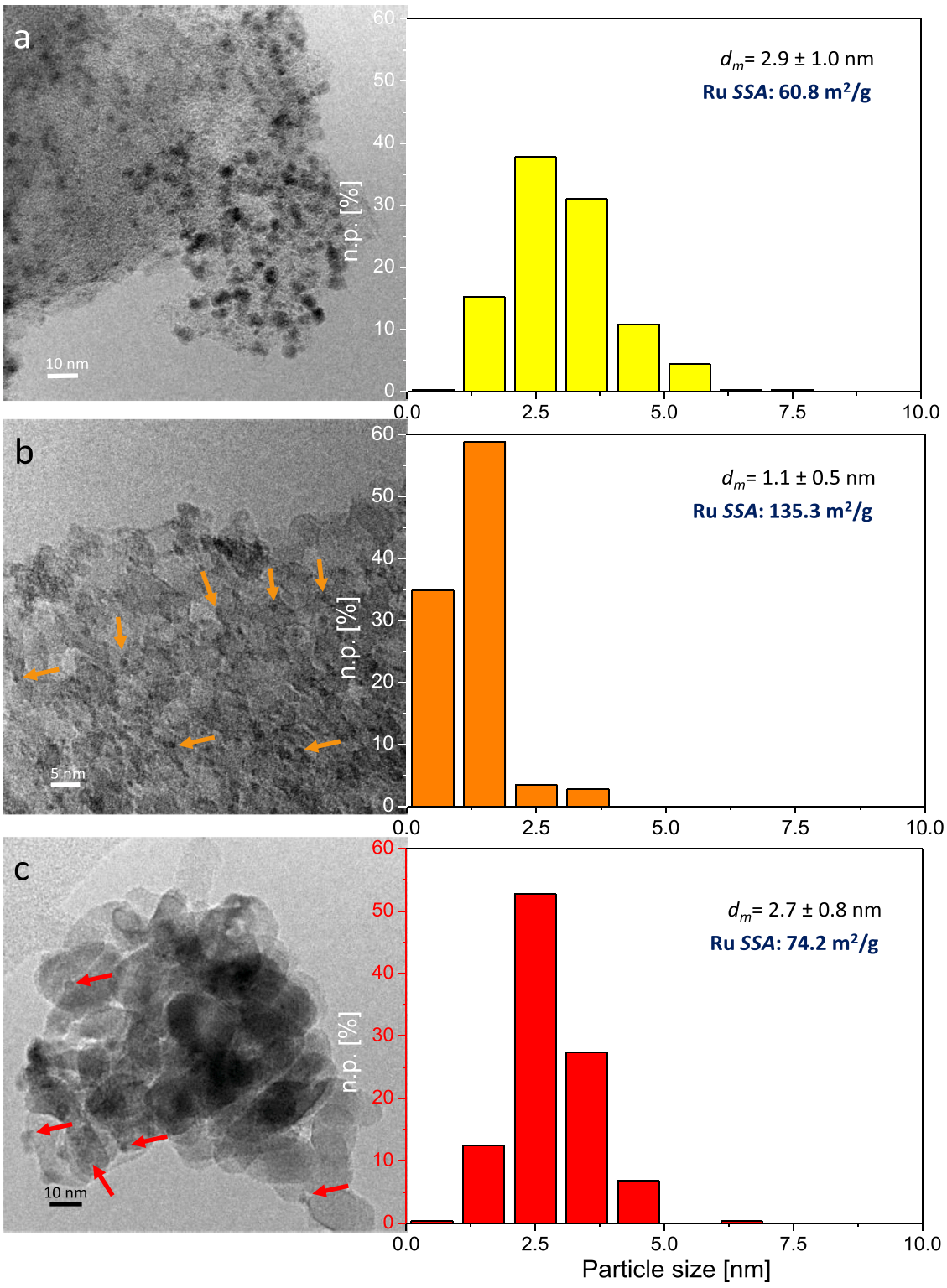

Fig. 2. TEM representative images and corresponding Ru particle size distribution of Ru/C (a), Ru/Al_2O_3 (b) and Ru/TiO_2 (c). The obtained Ru average diameters (d_m) and *SSA* are reported for each catalyst. The presence of Ru nanoparticles is highlighted by arrows, whereas n.p. [%] is the number of particles with diameter d_i. Instrumental magnification: 150,000× (a, and b) and 300,000× (c).

nanoparticles in air atmosphere were detected in the case of the Ru/TiO_2 catalyst (red line). Moreover, bands typical of anatase [44] and rutile [45] were also observed. Conversely, in the case of Ru/Al_2O_3 (orange line) only a broad band centered at 123,00 cm^{-1}, red shifted with respect to the absorptions displayed by Ru/TiO_2, and likely ascribed to $Ru^{\delta+}$ species was observed, according to the higher Ru dispersion obtained by TEM analysis.

3.2. MW-assisted sorbitol dehydration to isosorbide

According to the literature, a temperature range between 170 °C and 210 °C is usually the most adequate for isosorbide synthesis from

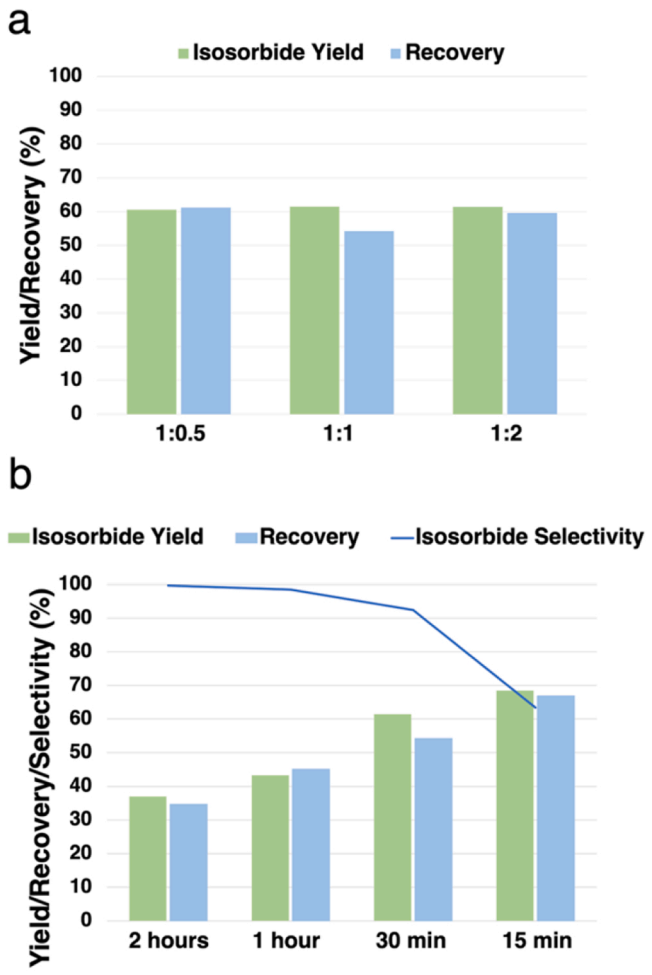

Fig. 3. Effect of (a) sorbitol:β zeolite ratio (190 °C, 30 min) and (b) time (190 °C, sorbitol:zeolite 1:1) on the sorbitol dehydration to isosorbide.

Table 1
Effect of temperature on sorbitol dehydration to isosorbide.[a].

Temperature	Conversion (%)	Selectivity (%)[b]	Recovery (%)	Isosorbide yield (%)
170 °C	97.8	62.0	68.1	59.6
190 °C	100	92.4	54.2	61.5
210 °C	100	97.5	43.4	40.7

aReaction conditions: 30 bar N_2, 30 min, sorbitol:H-β zeolite ratio 1:1).
bDetermined by GC-FID

sorbitol [6,24,46]. In this work, the MW-assisted neat sorbitol dehydration to isosorbide was preliminary carried out by using two commercial zeolites, zeolite H-Y (30:1 SiO_2:Al_2O_3) and H-β (360:1 SiO_2:Al_2O_3), and using different zeolite:sorbitol ratios at 190 °C, for 1 h (**Fig. SI-8**). In these conditions, the highest isosorbide yield was achieved in the presence of the H-β zeolite and with a zeolite:sorbitol weight ratio equal to 2:1. Indeed, β zeolites are considered an optimal choice in terms of size of the pores, as a paper by Jeong et al. has proved that the size of the sorbitol (5.7 Å) and isosorbide (6.2 Å) molecules is similar to that of their pores, which results in higher reactivity, compared to zeolites with smaller pores [46]. The role of H-β zeolites for isosorbide continuous-flow production has then been effectively observed [27,47].

With the adoption of shorter reaction times, it was observed that H-β zeolite:sorbitol ratio has not affected neither isosorbide yield nor percent recovery. (Fig. 3**a**). A 1:1 ratio has been chosen for the prosecution of the optimization process, to improve the mass transfer under neat conditions.

The effect of temperature on sorbitol dehydration is shown in Table 1, in which the results of sorbitol dehydration to isosorbide carried out at different temperatures for 30 min of reaction time are summarized.

A temperature of 170 °C guaranteed the highest recovery (61.5 %), but with a lower conversion, resulting in a 16.6 % selectivity towards 1,4-anhydrosorbitol, indicating an incomplete dehydration, according to Scheme 1. By increasing the temperature to 190 °C a 61.5 % isosorbide yield was obtained, conversely at 210 °C a 97.6 % selectivity towards isosorbide was achieved at the expenses of both recovery (43.4 %) and yield (40.7 %) due to the formation of humins [14].

After 190 °C has been chosen as the most adequate temperature, the same dehydration reaction has been performed with the use of 30Y zeolite, giving a 55.1 % yield towards isosorbide, along with a 66.7 % recovery and a complete conversion. Given the 63.9 % isosorbide selectivity, it is interesting to point out the consistent formation of sorbitan intermediates not involved in isosorbide formation mechanism (e.g. 1,5 and 2,5-anhydrosorbitol). The formation of undesired reaction intermediates and the generally lower isosorbide yields with low-Si:Al zeolites has been reportedly described in literature as a consequence of a promoted first dehydration step, after which the reactivity of the second dehydration step remains hindered [27]. On the other hand, the adoption of H-β zeolites with high Si:Al ratios and subsequently higher hydrophobicity has been observed to thermodynamically favor water elimination [24]. As a consequence of experimental and literature evidence [35,47,48], H-β zeolite offered more promising catalytic performances, compared with H-Y zeolite.

The effect of the reaction time on sorbitol dehydration is reported in Fig. 3**b**. Although complete sorbitol conversion was observed with each chosen reaction time, a 15-minute reaction has given an optimized 68.5 % isosorbide yield, along with a 66.9 % recovery. Compared with the work from Kobayashi and colleagues, the developed procedure has achieved a slightly lower isosorbide yield (76 % V 68.5 %) [24], operating a 8-times shorter reaction time, offering catalytic performances totally comparable with the majority of heterogeneous catalysts [6].

To further prove the predominant role of Brønsted acidity in sorbitol dehydration to isosorbide, the H-β zeolite has been soaked for 24 h in brine, causing H^+ protons to be replaced by Na^+ species. The resulting Na-β zeolite was then tested in sorbitol affording a poor conversion; moreover, neither isosorbide nor other intermediates were detected (**Fig. SI-9**), clearly demonstrating that the presence of Brønsted acid sites is necessary to dehydrate sorbitol.

The recyclability of H-β (360:1 SiO_2:Al_2O_3) and H-Y zeolite (30:1 SiO_2: Al_2O_3) was evaluated, basing on a calcination procedure described in literature (550 °C, 8 h) [24]. When employed in the optimized conditions for sorbitol dehydration (30 bar N_2, 15 min, 190 °C, sorbitol:zeolite 1:1), different behaviors regarding the two zeolites were observed. Since the first regeneration, the use of H-β zeolite did not result in any isosorbide formation, while H-Y zeolite was able to offer slightly decreasing isosorbide yield after four regeneration/recycling procedures (**Fig. SI-10**).

The differences regarding the recyclability of H-β and H-Y zeolite were investigated then determined with TPD analyses of ammonia and are reported in **Figs. SI-11b** and **SI-11c**. Following TPD characterization results, higher ammonia desorption from H-Y zeolite sites was observed, since NH3 desorption values for H-Y and H-β zeolite were respectively 732 μmol/g and 280 μmol/g. On the other hand, a marked contribution to the desorption peak at 700 °C (number 3) observed for H-β zeolite by H2O desorption upon Si–OH groups condensation can be hypothesized. The presence of Si–OH groups is directly correlated to the SiO_2: Al_2O_3 ratio [27], implying a higher number of silanol groups with an increasing Si content in the H-β zeolite structure. Given the conspicuous presence of Si–OH groups, water formation from silanol condensation promoted by MW could have contributed to the deactivation of H-β zeolite, that cannot be recovered after calcination.

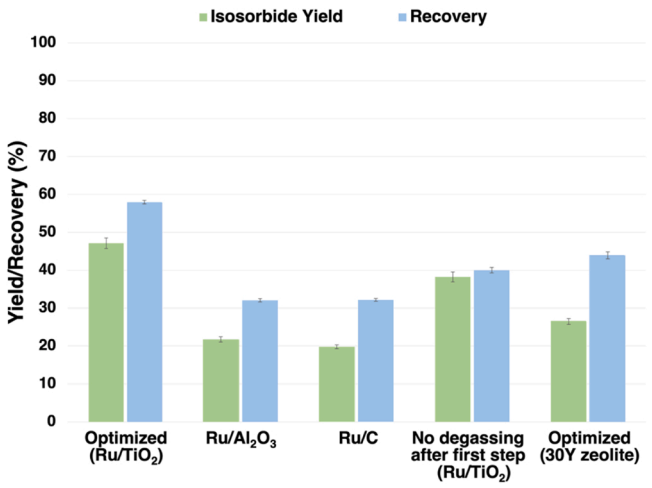

Fig. 4. Effect of different catalysts and j H_2 atmosphere on isosorbide yield. Reaction conditions: first step - 155 °C, 1 h, 40 bar H_2, glucose:H-β zeolite: catalyst ratio (4:4:1); second step – 190 °C, 30 min, 20 bar N_2.

Table 2
Effect of the time of the dehydration step[a].

Second step duration (min)	Conversion (%)	Selectivity (%)[b]	Isosorbide yield (%)	Recovery (%)
60	100	87.4	13.9	22.4
30	100	74.8	47.1	57.9
15	75.8	30,5	13.4	60.3

[a]First hydrogenation step performed at 155 °C, 40 bar H_2, 60 min, glucose:H-β zeolite:Ru/TiO_2 4:4:1.
[b]Determined with GC-FID

3.3. One-pot MW-assisted isosorbide production from glucose and reuse of catalysts

Both Ru/TiO_2 and Ru/Al_2O_3 were chosen to perform the one-pot MW assisted isosorbide production from glucose, as for these catalysts, yields and % recovery were higher (Fig. 1). The one-pot reaction was carried out using either H-β or H-Y zeolites; higher isosorbide yield was obtained when employing the former (47.1 % vs. 26.6 %), that was consequently employed for process optimization (Fig. 4). The lower isosorbide yield obtained with H-Y (30:1 SiO_2:Al_2O_3) can be imputed to the higher acidity of H-Y zeolite, compared with H-β (**Figs. SI-11b**, **SI-11c**), which lead to a lower overall isosorbide yield due to the formation of degradation products, such as humins.

Despite affording a higher sorbitol yield from glucose hydrogenation, Ru/Al_2O_3 led to lower recovery and isosorbide yield in the one-pot conversion, compared to Ru/TiO_2. The differences observed between the two catalysts can be traced back to the higher acidity observed for the Al_2O_3 support, that may have resulted in the promotion of side-reactions and consequent humins formation (Fig. 4).

Ru/C catalyst was also employed under optimized conditions, affording slightly lower yield than Ru/Al_2O_3 (19.8 % vs. 21.7 %). According to these results, all the subsequent one-pot optimization experiments (if not differently specified) involved the use of the Ru/TiO_2 catalyst and H-β zeolite.

The addition of the commercial zeolite to the reaction mixture after the hydrogenation step (Table 2) resulted (reaction time 1 h) in an isosorbide yield lower than that obtained after the single step MW-assisted sorbitol dehydration reported in **Fig. SI-8** (13.4 % and 52.5 %, respectively) after 1 h of reaction. However, the yields increased if the zeolite was added at the beginning of the one-pot reaction (32.8 %). This could be explained by a partial promotion of sorbitol dehydration already during the hydrogenation step.

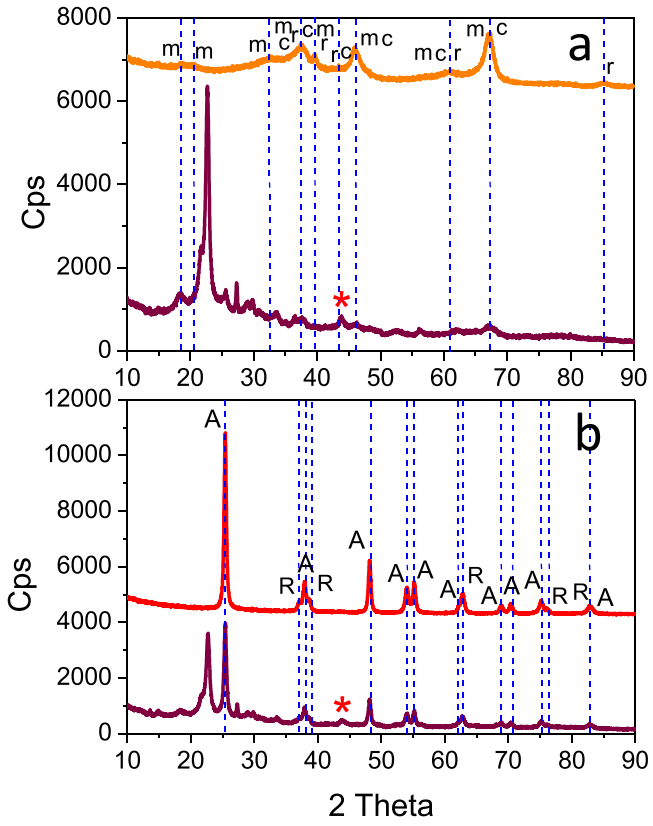

Fig. 5. XRD patterns of the Ru/Al_2O_3 fresh catalyst (orange line) and of the mixture of Ru/Al_2O_3 + H-β zeolite (purple line) after one-pot MW-assisted isosorbide production from glucose (a). m= monoclinic, c= cubics and r = rombohedral. (Reaction conditions, first glucose hydrogenation step: 155 °C, 1 h, 40 bar H_2; second sorbitol dehydration step: 190 °C, 30 min, 20 bar N_2). A glucose:H-β Zeolite:Ru/Al_2O_3 ratio equal to 4:4:1 was employed. XRD patterns of the Ru/TiO_2 fresh catalyst (red line) and of the mixture of Ru/TiO_2 + H-β zeolite (purple line) after one-pot MW-assisted isosorbide production from glucose (b). A= anatase, R= rutile. Reaction conditions, first glucose hydrogenation step: 155 °C, 1 h, 40 bar H_2; second sorbitol dehydration step: 190 °C, 30 min, 20 bar N_2). A glucose:H-β Zeolite:Ru/TiO_2 ratio equal to 4:4:1 was employed.

After the time required for glucose hydrogenation, the H_2 atmosphere was replaced by an inert atmosphere (N_2) to accomplish sorbitol dehydration. The catalyst:substrate ratio and temperature were the same as optimized in the single steps previously described. A longer reaction time had a negative effect on isosorbide yield and recovery, while shorter times led to an incomplete conversion of sorbitol (Table 2). Indeed, upon performing a 30 min dehydration step, the Ru/TiO_2-catalyzed one-pot reaction afforded an isosorbide yield of 47.1 %. Compared to the results of the single dehydration step, the lower isosorbide yield may be due to the deposition of glucose-derived humins on the acidic sites of the zeolite, causing a reactivity decrease. The obtained results represent the first reported development of a one-pot solvent-free procedure and the first zeolite-catalyzed procedure for direct isosorbide production from glucose. The one-pot reactions reported in Fig. 4 were carried out in triplicate.

The effect of the presence of a reactive atmosphere on the dehydration step was also studied, showing a slight decrease of isosorbide yield when no degassing was performed. This effect can be explained by the promotion of sorbitol hydrogenolysis in the presence of Ru-based catalysts at the correspondent reaction conditions obtained by maintaining the H_2 atmosphere (190 °C, 40 bar H_2) [49] (Fig. 4).

To get further insights on the parameters ruling the different

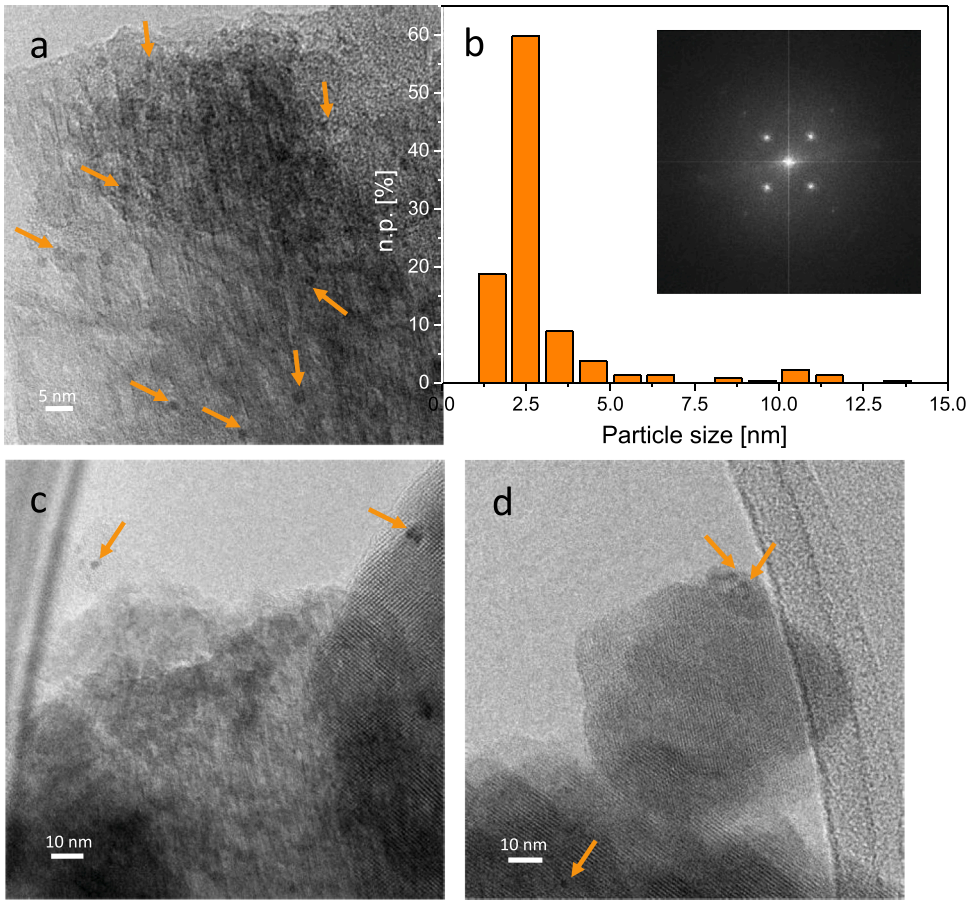

Fig. 6. TEM (a) and high-resolution TEM (c and) images of the Ru/Al_2O_3 + H-β zeolite catalysts after one-pot isosorbide synthesis from glucose. Ru particle size distribution and Fast Fourier Transform (FFT) of the image shown in a (b). The presence of Ru nanoparticles is highlighted by arrows, whereas n.p. [%] is the number of particles with diameter d_i. Instrumental magnification: 250,000× (a) and 150,000× (c and d). (Reaction conditions, first glucose hydrogenation step: 155 °C, 1 h, 40 bar H_2; second sorbitol dehydration step: 190 °C, 30 min, 20 bar N_2). The one-pot isosorbide synthesis from glucose was performed with a glucose:H-β Zeolite:Ru/Al_2O_3 ratio equal to 4:4:1.

catalytic performances displayed by the two catalysts in the one-pot MW-assisted isosorbide production from glucose, a detailed XRD characterization of the fresh catalysts as well as of the used mixtures of Ru/Al_2O_3 + H-β zeolite and Ru/TiO_2 + H-β zeolite catalysts was carried out. The results are summarized in Fig. 5**a** and 5**b**, respectively. Firstly, the commercial alumina support of the Ru/Al_2O_3 fresh catalyst (orange line) seems constituted by a mixture of monoclinic (m, JCPDS file number 00–011–0517), cubic (c, JCPDS file number 00–002–1420) and rombohedral (r, JCPDS file number 00–002–1373).

Moreover, likely due to the very low size of the Ru nanoparticles, no peaks ascribed to crystalline Ru were detected. However, beside the presence of peaks related to the alumina support and of the β zeolite (see also **Fig. SI-12**), the 101 peak related to hexagonal metallic Ru was clearly observed (and marked by a red asterisk) at 2 Theta around 44 in the pattern related to the of Ru/Al_2O_3 + H-β zeolite mixture after the MW-assisted one-pot reaction (purple line). This feature indicates that some Ru coalescence to form bigger crystalline nanoparticles occurred under reducing reaction conditions, as confirmed by TEM measurements carried out on the same mixture (Fig. 6), that revealed a broader particle size distribution (Fig. 6**b**) and average diameter $d_m = 2.9 \pm 2.1$ nm, resulting in a marked decrease of the Ru SSA to 51.44 m^2/g.

An analogous behavior as for the formation of metallic crystalline Ru after MW-assisted one-pot reaction was observed also in the case of Ru/TiO_2 (Fig. 7**b**). Indeed, the XRD pattern of the fresh Ru/TiO_2 catalyst (red line) revealed that the titania support is mainly made up by tetragonal anatase (A, JCPDS file number 00–001–0562) and in minor extent, by the tetragonal rutile phase (R, JCPDS file number 00–001–1292). Also in this case, no peaks related to crystalline Ru were present. Conversely, the 101 peak of hexagonal metallic Ru (red asterisk) was observed in the XRD pattern collected on the Ru/TiO_2 + H-β zeolite catalysts after one-pot isosorbide synthesis from glucose (purple line).

In addition, a particle size distribution broader than that of the fresh catalyst and an average Ru size of 3.0 ± 1.5 nm were obtained (Fig. 7**b**). An evident, even if less pronounced than in the case of Ru/Al_2O_3, decrease of the Ru *SSA* to 34.78 m^2/g was attained.

Overall, the TEM findings indicated that despite the observed decrease of Ru *SSA* for both catalysts, a large fraction of Ru nanoparticles still has size ≤ 2.5 nm without significant changes of Ru dispersion especially in the case of Ru/TiO_2. The spent catalytic mixtures were therefore recycled, and the results are shown in Table 3**.** It is worth noting that XRD and TEM measurements clearly pointed out the high stability of the two commercial supports and above all of the H-β zeolite under reaction conditions, as demonstrated by the presence of the corresponding peaks in the XRD patterns (Fig. 5) and by the presence of diffraction fringes in the high-resolution TEM images as well as of diffraction spots in the corresponding FFTs (Figs. 6**b**, 6**c** and 6**d** and 7).

TGA measurements were carried out on all catalysts before and after reaction, (**Figs. SI-13, SI-14**). It was found that Ru/C displayed the highest weight losses (−9,8 % and −18,3 % for the fresh and used catalyst, respectively). Overall, the weight loss of both fresh and used catalysts follows the order: $Ru/C > Ru/Al_2O_3 > Ru/TiO_2$, in agreement with the *SSA* of the supports (**Fig. SI-14**). Moreover, the weight losses of the catalysts after reaction were higher than those observed for the fresh catalysts. FTIR-ATR analyses (**Figs. SI-15**, **SI-16**) put in evidence the presence of bands assigned to CH stretching modes due to reactant/products species adsorbed on the catalyst surface upon reaction.

After a simple recycle (same conditions as the optimized one-pot reaction), 81.4 % glucose conversion was observed. However, a severely lower isosorbide yield was obtained (4.7 %) (Table 3). The analysis on the reaction mixture highlighted the presence of sorbitol, indicating that Ru/TiO_2 maintained its reactivity.

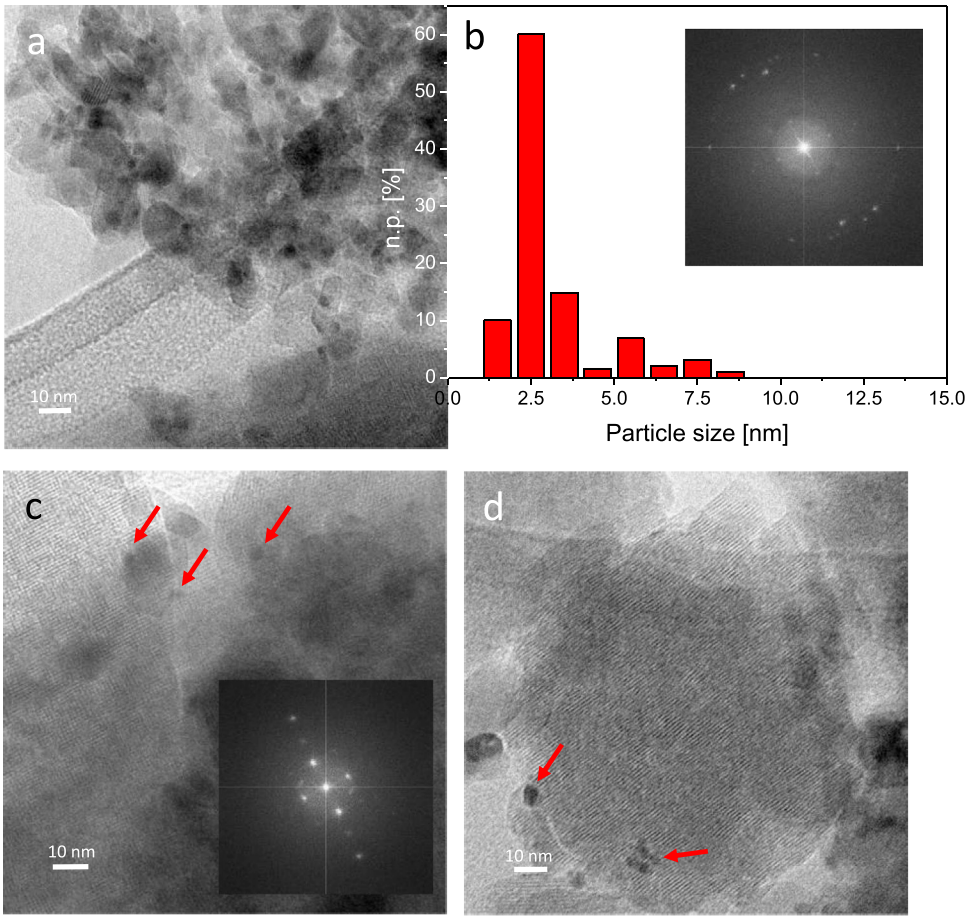

Fig. 7. High-resolution TEM (a, c and) images of the Ru/TiO_2 + H-β zeolite catalysts after one-pot isosorbide synthesis from glucose. Ru particle size distribution and Fast Fourier Transform (FFT) of the image shown in a (b). Inset: FFT of the image shown in c. The presence of Ru nanoparticles is highlighted by arrows, whereas n.p. [%] is the number of particles with diameter d_i. Instrumental magnification: 150,000×. (Reaction conditions, first glucose hydrogenation step: 155 °C, 1 h, 40 bar H_2; second sorbitol dehydration step: 190 °C, 2 h, 20 bar N_2). The one-pot isosorbide synthesis from glucose was performed with a glucose:H-β Zeolite:Ru/TiO_2 ratio equal to 4:4:1.

Table 3
Recycling tests[a].

Reaction	Conversion (%)	Isosorbide yield (%)	Recovery (%)
Optimized conditions (first run)	100	47.1	57.9
Simple Recycle	81.4	4.7	55.9
Recycle with fresh H-β zeolite addition (same amount of the first run)	100	46.0	41.6

aReaction conditions: first glucose hydrogenation step: 155 °C, 1 h, 40 bar H_2; second sorbitol dehydration step: 190 °C, 30 min, 20 bar N_2.

This hypothesis was confirmed by reuse tests regarding the sole hydrogenation step. Ru/TiO_2 afforded sorbitol yields up to 50 % after 3 runs, without any thermal treatment (Fig. 8). Ru/TiO_2 activity loss towards sorbitol from the first to the second cycle may be due to a lower Ru dispersion observed by HRTEM (Fig. 7) accompanied by the formation of crystalline Ru nanoparticles after hydrogenation reactions, which was observed by XRD and discussed in Fig. 5.

Consistently with the recycling issues already reported (Section 3.2), the need for a regeneration step for the zeolite system due to a coking-related loss of activity [14] required calcination of the spent catalytic mixture after the first use at 450 °C for 8, using a lower temperature than the one required for the sole zeolite regeneration, in order to avoid Anatase-Rutile transition [50].

The calcined catalytic mixture afforded a 77.9 % glucose conversion, along with the absence of isosorbide into the crude reaction, confirming the poor recyclability of the employed H-β.

More interesting reactivity results were obtained when adding again after the first cycle the same amount of fresh zeolite initially present in the reaction mixture. In this case, isosorbide yield did not change, confirming the reusability of the Ru/TiO_2 catalyst in a one-pot scenario (Table 3).

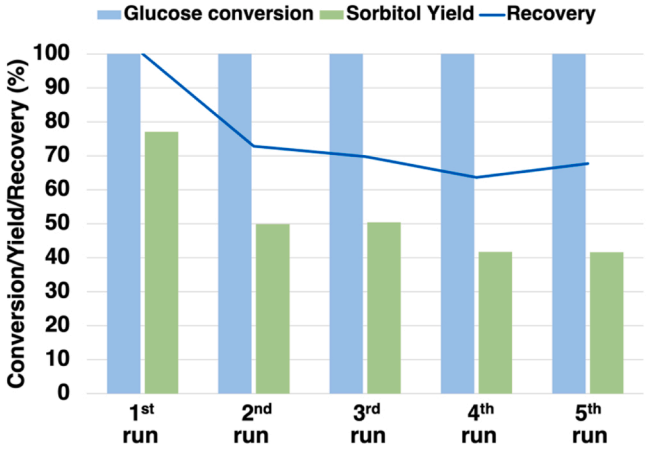

Fig. 8. Recycling tests for glucose hydrogenation reaction (Reaction conditions: 155 °C, 40 bar H_2, 1 h, glucose:catalyst ratio 4:1).

3.4. *One-pot MW-assisted cellulose conversion: preliminary studies*

The development of direct isosorbide production via cellulose conversion represents an appealing approach in the context of the development of a biorefinery [28]. However, solventless conditions cannot be exploited, due to cellulose degradation at high temperatures and mass

Table 4
Results for glucose CTH screening[a].

Catalyst	Conversion (%)	Hydrogenation products selectivity (%)[b,c]	Recovery (%)
Ru/C	100	81.3	57.9
Ru/TiO_2	100	0	55.9
Ru/Al_2O_3	100	0	41.6

[a]Reaction conditions: glucose:catalyst ratio 4:1, 200 °C, 4 h, 30 bar N2, 23 % w/w 2-propanol in water, glucose concentration 8.8 mg/mL. [b]Sorbitol and mannitol were detected in the reaction mixture.
[c]Determined with GC-FID

transfer limitations. On the other hand, water cannot be used as solvent, in order to not disfavor the dehydration step to isosorbide. The need of hydrolysis, hydrogenation and dehydration reactions requires multi-functional catalytic systems. With this scope, the presence of Ru/C as hydrogenation catalyst is ubiquitous in works treating isosorbide production from cellulose [28], affording isosorbide yields ranging from 17 % to 65 %. Despite these promising results, the reported processes use, along with Ru/C, catalysts that often require harsh reaction conditions or reaction times up to 24 h (e.g. heteropolyacids and mineral acids).

For these reasons, the authors decided to investigate the use of H-donors as both H_2 source and solvents to overcome mass transfer limits. In a previous work, the role of Ru/C and Ru/TiO_2 was investigated for Catalytic Transfer Hydrogenation (CTH) of levulinic acid to γ-valerolactone [40,51], with 2-propanol. Therefore, the produced Ru catalysts were firstly tested for glucose CTH, using 2-propanol as H_2 source. The obtained results are reported in Table 4, clearly showing the activity of Ru/C towards CTH, while the use of Ru/TiO_2 and Ru/Al_2O_3 did not result in hydrogenation products formation.

The role of formic acid towards cellulose hydrolysis [31], H_2 generation [33,5253] and partially towards sorbitol dehydration is known.

Based on the above reported and literature results, Ru/C was used to evaluate H_2 generation from formic acid investigating initially the one-pot conversion of glucose to isosorbide.

Basing on literature regarding CTH of glucose to sorbitol [54], pure formic acid was used, since the presence of water in the reaction could affect further sorbitol dehydration.

As previously reported [55], temperatures > 200 °C are required to weaken metal-H interactions and generate H_2. After a 2 h reaction at 200 °C, a 10.8 % recovery and a 28.2 % isosorbide selectivity were observed, proving the effective H_2 generation for glucose hydrogenation, along with the Brønsted acidity-promoted sorbitol dehydration.

Despite isosorbide formation, the progressive depletion of formic acid during the reaction led us to evaluate the addition of acidic zeolites (1:2 substrate:zeolite ratio) to boost dehydration step. The use of zeolites for cellulose depolymerization and glucose hydrogenation to sorbitol was reported previously [54]. Therefore, for optimization of the cellulose conversion conditions, H-Y with SiO_2:Al_2O_3 = 5 was chosen as the acidic catalyst, both to prompt cellulose hydrolysis and dehydration step, because of the higher acidity (**Figs. SI-11a**, **SI-11b**). Preliminary investigations on glucose conversion showed that with the use of a 1:2 glucose:zeolite ratio, higher recovery (28.8 %) and selectivity towards isosorbide (32.6 %) were observed. However, 26.6 % of levulinic acid was also observed, owing to the higher Brønsted acidity of H-Y (SiO_2:/Al_2O_3 = 5), leading to a different reaction pathway induced by an initial glucose isomerization reaction to fructose, via the formation of 5-HMF (5-Hydroxymethylfurfural) as intermediate (Scheme 2) [56].

Nevertheless, when cellulose was used as a substrate, better results were achieved (Fig. 9), with.

higher recovery (42.3 %) and selectivity (45.1 %). Consistently with the glucose-based reaction, recovery (18.1 %) and selectivity (15.3 %) were lower when the reaction was performed without the presence of H-Y zeolite with SiO_2:Al_2O_3 = 5. The differences regarding the glucose and the cellulose-based reactions can be traced back to degradation of the glucose itself.

Despite the promising results, isosorbide yield was low (2.5 %) thus requiring further investigation. The effects of H-Y with SiO_2:Al_2O_3 = 30 and H-β zeolite were also studied, affording lower isosorbide yields compared to those obtained for H-Y with SiO_2:Al_2O_3 equal to 5 (**Fig. SI-17**), as the presence of dehydration intermediates (e.g. 1,4-anhydrosorbitol) was detected. To improve the yields, a 4 h reaction time was investigated, leading to a 48.2 % recovery and a 2.7 % isosorbide yield. The slight enhancement of isosorbide yield may be ascribed to the occurrence of degradation reactions. The use of a more diluted solution of formic acid (50 %) in water afforded a 39.2 % recovery and 1.4 % isosorbide yield, proving the negative effect of water on sorbitol dehydration.

Considering the progressive formic acid consumption during the catalytic transfer hydrogenation reaction, lower isosorbide yield could be a consequence of a lack of H_2 produced in the system. Therefore, the reaction was carried out under a H_2 pressure of 20 bar, giving a final 48 % recovery and a 4.2 % isosorbide yield. A further H_2 pressure of 40 bar

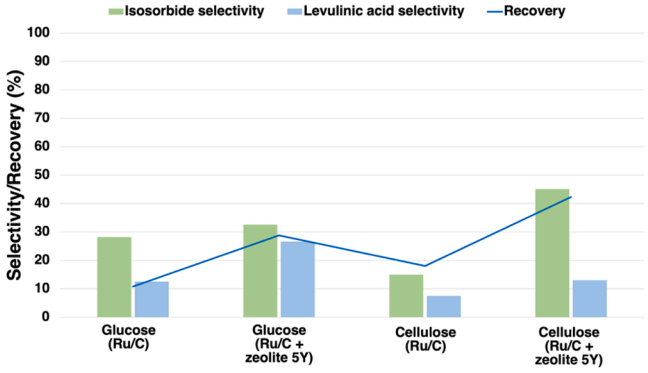

Fig. 9. Results for cellulose conversion to isosorbide. (Reaction conditions: 200 °C, 2 h, 30 bar N_2, 16.7 % substrate concentration in pure formic acid, 2.5:1 substrate:Ru/C ratio, 1:2 substrate:zeolite ratio). 5Y stands for H-Y with SiO_2:Al_2O_3 ratio equal to 5.

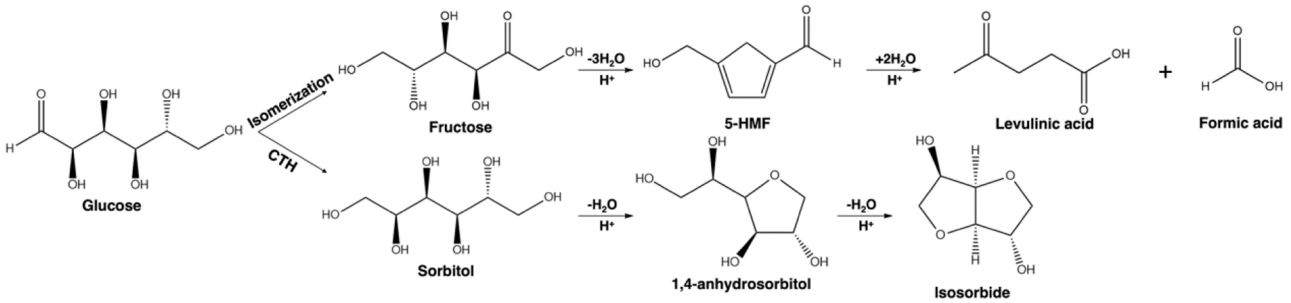

Scheme 2. Reaction pathways from cellulose-derived glucose towards levulinic acid (upper) and isosorbide (lower).

was investigated, affording a 2.08 % isosorbide yield, as a consequence of the overlapping reaction conditions of CTH and sorbitol hydrogenolysis [49]. The preliminarily optimized conditions reached were then tested with the presence of H-Y with SiO_2:Al_2O_3 = 30 and H-β zeolites, resulting in a lower recovery (24.2 % for the former zeolite and 15.4 % for the latter) and a 2.1 % yield for H-Y with SiO_2:Al_2O_3 = 30, due to the milder acidity. Regarding H-β zeolites, the observed isosorbide value was comparable with that obtained in the presence of H-Y with SiO_2:Al_2O_3 = 5 (4.1 %).

Ru/TiO_2 and Ru/Al_2O_3 were finally tested in the same conditions of Ru/C. While with the use of Ru/TiO_2 the formation of isosorbide was not observed, Ru/Al_2O_3 afforded a 32.9 % recovery and a 2.4 % isosorbide yield, confirming the role of Ru/C as the most adequate catalyst for this process.

These preliminary results highlight the need for further investigations aiming to optimize every single step of cellulose conversion. With the scope of using a single catalytic system for both the CTH and dehydration, dual-function catalysts would represent a promising approach for the production of isosorbide from cellulose [28].

4. Conclusions

The MW-assisted one-pot isosorbide catalytic synthesis was investigated, with the development of a solvent-free procedure with the use of glucose as starting material. The combined catalytic synergy of Ru-based catalysts and acidic zeolites was exploited, and a 47.1 % isosorbide yield was obtained with the use of Ru/TiO_2 and H-β Zeolite. An extent characterization regarding fresh and used catalysts was carried out with a multi-technique approach, and the Ru/TiO_2 catalyst maintained > 50 % sorbitol yields after 4 cycles. The values observed for isosorbide yield from direct glucose conversion were maintained after fresh H-β Zeolite was added to the used catalytic mixture.

Direct cellulose conversion to isosorbide was also preliminarily investigated, with the use of formic acid as stoichiometric acid for cellulose hydrolysis and H-Donor. Despite the low yields obtained, the production of isosorbide with good selectivity occurred from a process avoiding the use of the fossil derived molecular H_2, a promising result for future improvements of reaction conditions and catalytic systems.

CRediT authorship contribution statement

Marco Belluati: Investigation, Writing- Original draft preparation. **Silvia Tabasso**: Conceptualization, Writing- Reviewing and Editing, Visualization. **Fabio Bucciol**: Investigation, Methodology. **Tommaso Tabanelli**: Resources, Investigation. **Fabrizio Cavani**: Validation, Methodology. **Giancarlo Cravotto**: Data curation, Methodology. **Maela Manzoli**: Conceptualization, Writing- Reviewing and Editing, Supervision.

Declaration of Competing Interest

The authors declare that they have no known competing financial interests or personal relationships that could have appeared to influence the work reported in this paper.

Data availability

No data was used for the research described in the article.

Acknowledgements

The Unversity of Turin (Ricerca Locale 2022) is acknowledged for the financial support.

Appendix A. Supporting information

Supplementary data associated with this article can be found in the online version at doi:10.1016/j.cattod.2023.114086.

References

[1] R.A. Sheldon, I. Arends, U. Hanefeld, Green Chemistry and Catalysis Physics, Technology, Applications. 2007.
[2] T. Werpy, G. Petersen. Volume I - Results of Screening for Potential Candidates from Sugars and Synthesis Gas, Top Value Added Chemicals from Biomass, 2004.
[3] J. Li, H.S.M.P. Soares, J.A. Moulijn, M. Makkee, Simultaneous hydrolysis and hydrogenation of cellobiose to sorbitol in molten salt hydrate media, Catal. Sci. Technol. 3 (2013) 1565–1572.
[4] J.J. Bozell, G.R. Petersen, Technology development for the production of biobased products from biorefinery carbohydrates - The US Department of Energy's "top 10″ revisited, Green. Chem. 12 (2010) 539–554.
[5] Research and Markets, Isosorbide - Global Market Trajectory & Analytics (2022), https://www.researchandmarkets.com/reports/5140954/isosorbide-global-strategic-business-report.
[6] F. Delbecq, M.R. Khodadadi, D. Rodriguez Padron, R. Varma, C. Len, Isosorbide: recent advances in catalytic production, Mol. Catal. 482 (2020), 110648.
[7] G. Flèche, M. Huchette, Isosorbide preparation, properties and chemistry, Starch 38 (1986) 26–30.
[8] D.J. Saxon, A.M. Luke, H. Sajjad, W.B. Tolman, T.M. Reineke, Next-generation polymers: isosorbide as a renewable alternative, Prog. Polym. Sci. 101 (2020), 101196.
[9] F. Aricò, Isosorbide as biobased platform chemical: recent advances, Curr. Opin. Green. Sustain. Chem. 21 (2020) 82–88.
[10] P.A. Lazaridis, S. Karakoulia, A. Delimitis, S.M. Coman, V.I. Parvulescu, K. S. Triantafyllidis, D-Glucose hydrogenation/hydrogenolysis reactions on noble metal (Ru, Pt)/activated carbon supported catalysts, Catal. Today 257 (2015) 281–290.
[11] A. Aho, S. Roggan, O.A. Simakova, T. Salmi, D.Y. Murzin, Structure sensitivity in catalytic hydrogenation of glucose over ruthenium, Catal. Today 241 (Part B) (2015) 195–199.
[12] M.J. Ahmed, B.H. Hameed, Hydrogenation of glucose and fructose into hexitols over heterogeneous catalysts: a review, J. Taiwan Inst. Chem. Eng. 96 (2019) 341–352.
[13] H. Kobayashi, A. Fukuoka, Synthesis and utilisation of sugar compounds derived from lignocellulosic biomass, Green. Chem. 15 (2013) 1740–1763.
[14] C. Dussenne, T. Delaunay, V. Wiatz, H. Wyart, I. Suisse, M. Sauthier, Synthesis of isosorbide: an overview of challenging reactions, Green. Chem. 19 (2017) 5332–5344.
[15] A. De La Hoz, A. Loupy, Microwaves in Organic Synthesis, 3rd Edition. (2012).
[16] A. Yamaguchi, N. Mimura, M. Shirai, O. Sato, Kinetic analyses of intramolecular dehydration of hexitols in high-temperature water, Carbohydr. Res. 487 (2020), 107880.
[17] K.M. Mathew, S. Ravi, D. Padmanabhan, V.K.P. Unny, N. Sivaprasad, A rapid microwave assisted synthesis of [U-^{14}C] isosorbide and Dimethyl [U-^{14}C] isosorbide from D-[U-^{14}C] glucose, J. Label. Compd. Radio. 49 (2006) 333–337.
[18] C. Gozlan, E. Dereuer, M. Duclos, V. Molinier, J. Aubry, A. Redl, N. Duguet, M. Lemaire, Preparation of amphiphilic sorbitan monoethers through hydrogenolysis of sorbitan acetals and evaluation as bio-based surfactants, Green. Chem. 18 (2016) 1994–2004.
[19] P. Barbaro, F. Liguori, C. Moreno-Marrodan, Selective direct conversion of C5 and C6 sugars to high added-value chemicals by a bifunctional, single catalytic body, Green. Chem. 18 (2016) 2935–2940.
[20] M.R. Kamaruzaman, X.X. Jiang, X. De Hu, S.Y. Chin, High yield of isosorbide production from sorbitol dehydration catalysed by Amberlyst 36 under mild condition, Chem. Eng. J. 388 (2020), 124186.
[21] M.J. Ginés-molina, R. Moreno-tost, J. Santamaría-González, P. Maireles-torres, Dehydration of sorbitol to isosorbide over sulfonic acid resins under solvent-free conditions, Appl. Catal. A, Gen. 537 (2017) 66–73.
[22] A.A. Dabbawala, S.M. Alhassan, D.K. Mishra, J. Jegal, J.S. Hwang, Solvent free cyclodehydration of sorbitol to isosorbide over mesoporous sulfated titania with enhanced catalytic performance, Mol. Catal. 454 (2018) 77–86.
[23] A.A. Dabbawala, D.K. Mishra, G.W. Huber, J. Hwang, Role of acid sites and selectivity correlation in solvent free liquid phase dehydration of sorbitol to isosorbide, Appl. Catal. A, Gen. 492 (2015) 252–261.
[24] H. Kobayashi, H. Yokoyama, B. Feng, A. Fukuoka, Dehydration of sorbitol to isosorbide over H-beta zeolites with high Si/Al ratios, Green. Chem. 17 (2015) 2732–2735.
[25] Y. Zhang, C. Li, Z. Du, X. Chen, C. Liang, Dehydration of sorbitol into isosorbide over silver-exchanged phosphotungstic acid catalysts, Mol. Catal. 458 (2018) 19–24.
[26] M. Kurszewska, E. Skorupowa, J. Madaj, A. Konitz, W. Wojnowski, A. Wiśniewski, The solvent-free thermal dehydration of hexitols on zeolites, Carbohydr. Res. 337 (2002) 1261–1268.
[27] F. Brandi, I. Khalil, M. Antonietti, M. Al-Naji, Continuous-flow production of isosorbide from aqueous-cellulosic derivable feed over sustainable heterogeneous catalysts, ACS Sustain. Chem. Eng. 9 (2021) 927–935.

[28] I. Bonnin, R. Mereau, T. Tassaing, K. de Oliveira Vigier, One-pot synthesis of isosorbide from cellulose or lignocellulosic biomass: a challenge ? Beilstein J. Org. Chem. 16 (2020) 1713–1721.
[29] P. Sun, X. Long, H. He, C. Xia, F. Li, Conversion of cellulose into isosorbide over bifunctional ruthenium nanoparticles supported on niobium phosphate, ChemSusChem 6 (2013) 2190–2197.
[30] A. Shrotri, H. Kobayashi, A. Fukuoka, Cellulose depolymerization over heterogeneous catalysts, Acc. Chem. Res. 51 (2018) 761–768.
[31] L. Kupiainen, J. Ahola, Kinetics of formic acid-catalyzed cellulose hydrolysis, Biores 9 (2014) 2645–2658.
[32] M. Oregui-bengoechea, I. Gandarias, P.L. Arias, T. Barth, Unraveling the role of formic acid and the type of solvent in the catalytic conversion of lignin: a holistic approach, ChemSusChem 10 (2017) 754–766.
[33] V.V. Chesnokov, P.P. Dik, A.S. Chichkan, Formic acid as a hydrogen donor for catalytic transformations of tar, Energies 13 (2020) 4515.
[34] N. Yan, C. Zhao, C. Luo, P.J. Dyson, H. Liu, Y. Kou, One-step conversion of cellobiose to C6-alcohols using a ruthenium nanocluster catalyst, J. Am. Chem. Soc. 128 (2006) 8714–8715.
[35] F. Brandi, M. Al-Naji, Sustainable sorbitol dehydration to isosorbide using solid acid catalysts: transition from batch reactor to continuous-flow system, ChemSusChem 15 (2022), e202102525.
[36] F. Brandi, M. Bäumel, V. Molinari, I. Shekova, I. Lauermann, T. Heil, M. Antonietti, M. Al-Naji, Nickel on nitrogen-doped carbon pellets for continuous-flow hydrogenation of biomass-derived compounds in water, Green. Chem. 22 (2020) 2755–2766.
[37] Yu Sun, A.A. 2013, Glucose and cellobiose adsorption onto activated carbon, Publication No. 1547815, Public dissertation, Indiana University of Pennsylvania (2013).
[38] I. Bonnin, T. Tassaing, K.D.O. Vigier, Hydrogenation of sugars to sugar alcohols in the presence of a recyclable Ru/Al_2O_3 catalyst commercially available, ACS Sustain. Chem. Eng. 9 (2021) 9240–9247.
[39] A. Romero, E. Alonso, A. Nieto-Màrquez, Conversion of biomass into sorbitol: cellulose hydrolysis on MCM-48 and D -Glucose hydrogenation on Ru / MCM-48, Micro Mesopor. Mat. 224 (2016) 1–8.
[40] G. Grillo, M. Manzoli, F. Bucciol, S. Tabasso, T. Tabanelli, F. Cavani, G. Cravotto, Hydrogenation of levulinic acid to γ - Valerolactone via green microwave-assisted reactions either in continuous flow or solvent- free batch processes, Ind. Eng. Chem. Res. 60 (2021) 16756–16768.
[41] J. De Maron, L. Bellotti, A. Baldelli, A. Fasolini, N. Schiaroli, C. Lucarelli, F. Cavani, T. Tabanelli, Evaluation of the catalytic activity of metal phosphates and related oxides in the ketonization of propionic acid, Sustain. Chem. 3 (2022) 58–75.
[42] S. Cisneros, S. Chen, T. Diemant, J. Bansmann, A. Abdel-Mageed, M. Goepel, S. Olesen, E. Welter, M. Parlinska-Wojtan, R. Gläser, I. Chorkendorff, R. Jürgen Behm, Effects of SiO2-doping on high-surface-area Ru /TiO2 catalysts for the selective CO methanation, Appl. Catal. B Environ. 282 (2020), 119483.
[43] V. Ravat, P. Aghalayam, Effect of noble metals deposition on the catalytic activity of MAPO-5 catalysts for the reduction of NO by CO, Appl. Catal. A, Gen. 389 (2010) 9–18.
[44] X. Lin, K. Yang, R. Si, X. Chen, W. Dai, X. Fu, Photo-assisted catalytic methanation of CO in H_2-rich stream, Appl. Catal. B, Environ 147 (2014) 585–591.
[45] M. Du, J. Huang, D. Sun, D. Wang, Q. Li, High catalytic stability for CO oxidation over Au/TiO_2 catalysts by cinnamomum camphora leaf extract, Ind. Eng. Chem. Res. 57 (2018) 14910–14914.
[46] S. Jeong, K.J. Jeon, Y.K. Park, B.J. Kim, K.H. Chung, S.C. Jung, Catalytic properties of microporous zeolite catalysts in synthesis of isosorbide from sorbitol by dehydration, Catalysts 10 (2020) 1–12.
[47] M. Caiti, G. Tarantino, C. Hammond, Developing a Continuous process for isosorbide production from renewable sources, ChemCatChem 12 (2020) 6393–6400.
[48] R. Otomo, T. Yokoi, T. Tatsumi, Synthesis of isosorbide from sorbitol in water over high-silica aluminosilicate zeolites, Appl. Catal. A, Gen. 505 (2015) 28–35.
[49] A.M. Ruppert, K. Weinberg, R. Palkovits, Hydrogenolysis goes bio: from carbohydrates and sugar alcohols to platform chemicals, Angew. Chem. Int. 51 (2012) 2564–2601.
[50] N. Wetchakun, B. Incessungvorn, K. Wetchakun, S. Phanichphant, Influence of calcination temperature on anatase to rutile phase transformation in TiO_2 nanoparticles synthesized by the modified sol–gel method, Mater. Lett. 82 (2012) 195–198.
[51] M.G. Al-Shaal, R.H. Wright, R. Palkovits, Exploring the ruthenium catalysed synthesis of γ-valerolactone in alcohols and utilisation of mild solvent-free reaction conditions, Green. Chem. 14 (2012) 1260–1263.
[52] T.C. Johnson, D.J. Morris, M. Wills, Hydrogen generation from formic acid and alcohols using homogeneous catalysts, Chem. Soc. Rev. 39 (2010) 81–88.
[53] F. Bucciol, S. Tabasso, G. Grillo, F. Menegazzo, M. Signoretto, M. Manzoli, G. Cravotto, Boosting levulinic acid hydrogenation to value-added 1,4-pentanediol using microwave-assisted gold catalysis, J. Catal. 380 (2019) 267–277.
[54] B. Garc, A. Orozco-saumell, L. Manuel, J. Moreno, J. Iglesias, Catalytic transfer hydrogenation of glucose to sorbitol with raney ni catalysts using biomass-derived diols as hydrogen donors, ACS Sustain. Chem. Eng. 9 (2021) 14857–14867.
[55] X. Jin, B. Yin, Q. Xia, T. Fang, J. Shen, L. Kuang, C. Yang, Catalytic transfer hydrogenation of biomass-derived substrates to value-added chemicals on dual-function catalysts: opportunities and challenges, ChemSusChem 12 (2019) 71–92.
[56] S. Tabasso, E. Montoneri, D. Carnaroglio, M. Caporaso, G. Cravotto, Microwave-assisted flash conversion of non-edible polysaccharides and post-harvest tomato plant waste to levulinic acid, Green. Chem. 16 (2014) 73–76.